Two-dimensional mechanism of electrical conductivity in $Gd_{1-x}Ce_xBa_2Cu_3O_{7-\delta}$

2008 J. Phys.: Condens. Matter 20 345221

(http://iopscience.iop.org/0953-8984/20/34/345221)

J. Phys.: Condens. Matter **20** (2008) 345221 (5pp) doi:10.1088/0953-8984/20/34/345221

Two-dimensional mechanism of electrical conductivity in $Gd_{1-x}Ce_xBa_2Cu_3O_{7-\delta}$

S Mofakham, M Mazaheri and M Akhavan[1]

Magnet Research Laboratory (MRL), Department of Physics, Sharif University of Technology, PO Box 11365-9161, Tehran, Iran

E-mail: akhavan@sharif.edu

Received 18 December 2007, in final form 30 June 2008
Published 6 August 2008
Online at stacks.iop.org/JPhysCM/20/345221

Abstract

Partial substitutions of Pr and Ce are known to suppress the superconducting state in $REBa_2Cu_3O_{7-\delta}$ systems. We have substituted Ce for Gd in $Gd_{1-x}Ce_xBa_2Cu_3O_{7-\delta}$ compounds with $x = 0.0$–0.6 by the standard solid-state reaction technique. X-ray diffraction (XRD) experiments are performed and their results are refined by the Rietveld method. XRD analysis shows a predominantly single-phase perovskite structure with few impurity phases. Our resistivity results show that, by increasing the Ce content, T_c decreases, the transition temperature width increases, and in the normal state a metal–insulator transition (MIT) occurs at $x_c = 0.12$. The normal state resistivity of the samples and their slopes change at this point. The normal state resistivity of the samples is fitted with the variable range hopping (VRH) and the Coulomb gap (CG). Our results are most consistent with the two-dimensional VRH model.

1. Introduction

Since the discovery of $YBa_2Cu_3O_{7-\delta}$ (Y123), a great deal of effort has been made to explain the mechanism responsible for superconductivity in these systems. It is well known that different rare-earth ions can be substituted for yttrium ions in Y123, giving superconductivity with nearly the same critical temperature, $T_c = 92$ K, and superconducting properties. There are four exceptions to this case: RE = Pm, Pr, Tb and Ce. No investigation has been reported for the Pm123 compound because the Pm nucleus is radioactive and unstable [1]. The Pr123 compound is the only one which is isostructural with Gd123 but is not a superconductor [2]. As the Pr concentration is increased in $Gd_{1-x}Pr_xBa_2Cu_3O_{7-\delta}$ (GdPr123), T_c decreases monotonically. Then, the superconducting state vanishes at a concentration of $x = 0.45$ and the electrical behavior of the normal state also undergoes a transition from metallic to semiconducting phase at $x = 0.45$ [3]. The role of Pr substitution in the high temperature superconductors (HTSC) has been reviewed by Akhavan [4], and consideration of the Pr substitution for Gd and Ba in Gd123 has been extended in [5–7].

For RE = Tb and Ce, RE123 does not form in the 123 orthorhombic structure. Both Ce and Tb form double oxides $BaCeO_3$ and $BaTbO_3$, respectively, which lead to the formation of multiphase samples [1, 7, 8]. Ce, Tb and Pr have stable composition in the tetravalent state. Substitution of Ce and Pr for Y in Y123 films has shown a similar decrease in T_c with increasing rare-earth concentration [9]. In contrast, the Tb substitution for Y in Y123 has no appreciable effects on the T_c of thin films. Indeed, Ce and Tb rarely appear in the trivalent state and do not form a stable 123 phase structure. It has been demonstrated that the effective ionic radius of the trivalent element is important for the formation of the 123 phase; the phase becomes unstable when it is too large (La) or too small (Lu) [10]. On the basis of this ionic radius argument, the 123 phase should exist for Ce and Tb: however, it does not exist for Ce and Tb. One can attribute this observation to the failure of Ce and Tb to appear in their trivalent state.

In this work, we have studied the effect of Ce partial substitution for Gd in Gd123 compounds. XRD analysis is applied to prove the purity of the compounds and also to determine its crystalline structure. A superconducting transition is observed until $x = 0.6$ in order to investigate whether Ce destroys superconductivity through hole filling in the CuO_2 planes.

[1] Author to whom any correspondence should be addressed.

2. Experimental details

$Gd_{1-x}Ce_xBa_2Cu_3O_{7-\delta}$ (GdCe123) samples with $x = 0.0$, 0.03, 0.05, 0.09, 0.1, 0.12, 0.15, 0.3, 0.325, 0.35, 0.375, 0.4, 0.5, 0.6, 0.7, 0.8, 0.9 and 1 were synthesized by the standard solid-state reaction technique. Appropriate amounts of high purity (more than 99.9%) Gd_2O_3, CeO_2, $BaCO_3$ and CuO were mixed and calcined at 850 °C in air for 24 h. The same process was repeated at least twice in order to improve the homogeneity of the samples.

The powders were reground, and subsequently pressed into pellets and sintered at 950 °C for 24 h in flowing oxygen. In the cooling part, the samples were cooled to 650, 600 and 550 °C and retained under oxygen flow for 10 h each. These steps were required to improve the sample oxygen content. The samples were then slowly furnace cooled during 10 h to room temperature. The crystal structure of the samples was investigated by the XRD technique, using a Philips Xpert system with Co Kα_1 target ($\lambda = 1.7890$ Å). The XRD results have been analyzed by MAUD software based on the Rietveld method. An ac four-probe method with $f = 33$ Hz was used for the conductivity measurements of the samples within the temperature range from 10 to 300 K. The size of the samples was about $10 \times 3 \times 1$ mm^3 and the electrical leads were attached on the long side of the samples by silver paste. A Lake Shore-330 temperature controller with a Pt-100 resistor and GaAs diode were used for indicating and controlling the temperature, respectively. Different currents from 10 to 100 mA were applied in the conductivity measurements.

3. Results and discussion

The cuprate superconductors like Gd123 have a triple perovskite structure which possesses a structure constructed from three oxygen-deficient perovskite blocks stacked upon each other. The general formula for the perovskite structure is ABO_3. For Gd123 compounds Gd, Ba and any other doped ions belong to the A-site $\langle r_A \rangle$ and Cu ions belong to the B-site $\langle r_B \rangle$. The observed evolution of the structure with Ce doping of level x should be associated with the average ionic radius of the A-site cation ($r_A = (1-x)r_{Gd}/3 + xr_{Ce}/3$). This is related to the tolerance factor t [$t = ((1-x)r_{Gd}/3 + xr_{Ce}/3 + r_O)/\sqrt{2}(r_{Cu} + r_O)$], where r_i (i = Gd, Ce, Ba, Cu and O) represent the average ionic size of the element. The tolerance factor increases from 0.867 34 for $x = 0.0$–0.873 71 for $x = 0.6$ which implies that the samples have the orthorhombic structure.

The room temperature XRD spectra of the GdCe123 samples with $x = 0.0$, 0.1, 0.3 and 0.5 are shown in figure 1. The XRD patterns are analyzed using the standard Rietveld technique. By the XRD analysis, the 123 orthorhombic phase is found for all of the compounds and the main orthorhombic peaks responsible for the superconducting state are determined in figure 1. The (200) and (020) peaks near $2\theta \sim 55°$ for both the $x = 0$ and 0.1 samples are characteristic of the existence of the orthorhombic phase.

The superconductivity arises clearly from the $RBa_2Cu_3O_{7-\delta}$ phase. For the Pr-doped Y123 system, the XRD results

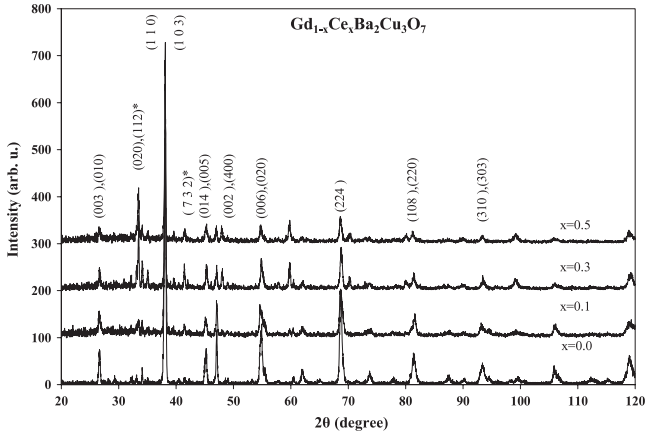

Figure 1. XRD spectra of $Gd_{1-x}Ce_xBa_2Cu_3O_{7-\delta}$ samples with $x = 0$, 0.1, 0.3 and 0.5. The stars (*) indicate the impurity phase of $BaCeO_3$.

reveal that the system has the orthorhombic structure with no secondary phase peaks [11] but for the Ce-doped samples there are some limitations: Cao *et al* [8] have synthesized the single-phase $Nd_{1-x}Ce_xBa_2Cu_3O_{7-\delta}$ (NdCe123) thin films up to $x = 0.35$ with the orthorhombic structure. Also, the $Y_{1-x}Ce_xBa_2Cu_3O_{7-\delta}$ (YCe123) thin films which have been prepared by Fincher *et al* [9] show a single phase with the orthorhombic structure for $x \leqslant 0.3$. Using the pulsed laser-ablation technique, Gnanasekar *et al* [10] have been successful in synthesizing the $Lu_{1-x-z}Ce_xCa_zBa_2Cu_3O_{7-\delta}$ (LuCeCa123) thin films which show a single phase up to the concentrations of $x = 0.15$ and $z = 0.15$.

The peak intensity of the Gd123 systems is affected by the Ce doping in which the intensity of the superconducting peaks for the pure samples is larger than the intensity of the superconducting peaks in the doped samples. Comparing the XRD spectra of the Pr-doped and the Ce-doped systems, it can be inferred that the GdCe123 samples with $x = 0.0$ and 0.1 contain no secondary phases but the samples including higher concentrations ($x > 0.1$) of the Ce ions contain secondary phases such as $BaCeO_3$ and $BaCuO_2$. The existence of these secondary phases suppresses the superconducting state in the GdCe123 systems, while for the GdPr123 systems which have no secondary phase other mechanisms should be considered for the suppression of superconductivity. In the GdCe123 samples with $x = 0.3$ and 0.5, the amount of the $BaCeO_3$ and $BaCuO_2$ impurity phases is less than 5%. The number and height of the secondary peaks such as (020) and (112), related to $BaCeO_3$ at $2\theta_B = 34°$, increase as x increases but the 123 phase is still the dominant phase even at $x = 0.5$.

The XRD pattern of the samples can be indexed by an orthorhombic lattice with space group $Pmmm$. The lattice parameters a, b and c, and the cell volume V are obtained from the x-ray diffraction of GdCe123 and are plotted in figure 2 as a function of Ce content. The a, b, V and orthorhombic distortion ($(a-b)/(a+b) \times 100\%$) parameters are found to decrease continuously with the increase of x while the c parameter increases.

The resistivity data $\rho(T)$ as a function of x for GdCe123 are represented in figure 3. Substitution of Ce has

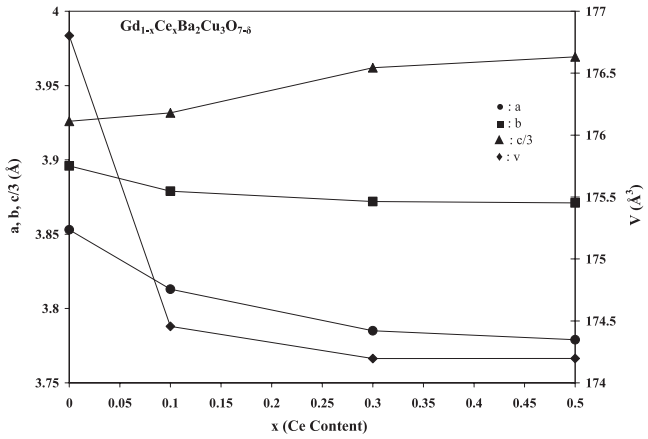

Figure 2. The lattice parameters a, b and c, and the cell volume V versus x.

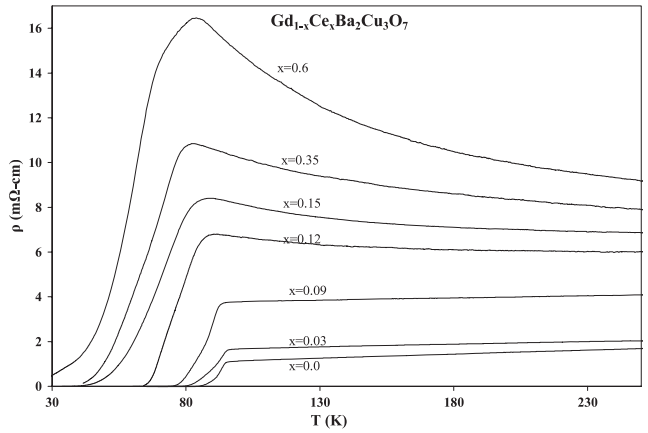

Figure 3. The resistivity versus temperature for the $Gd_{1-x}Ce_xBa_2Cu_3O_{7-\delta}$ compounds.

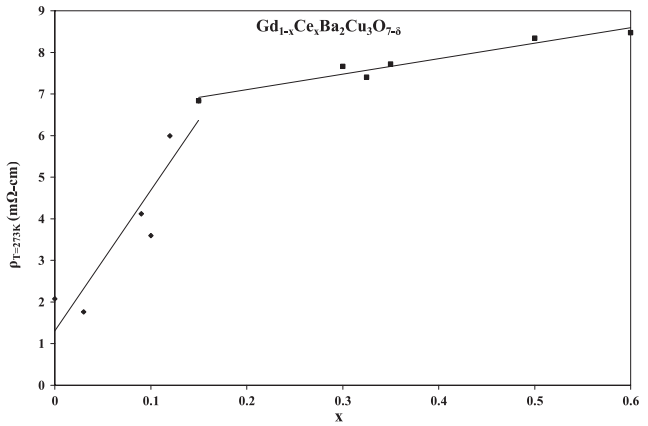

Figure 4. The normal state resistivity of the samples at $T = 273$ K versus x.

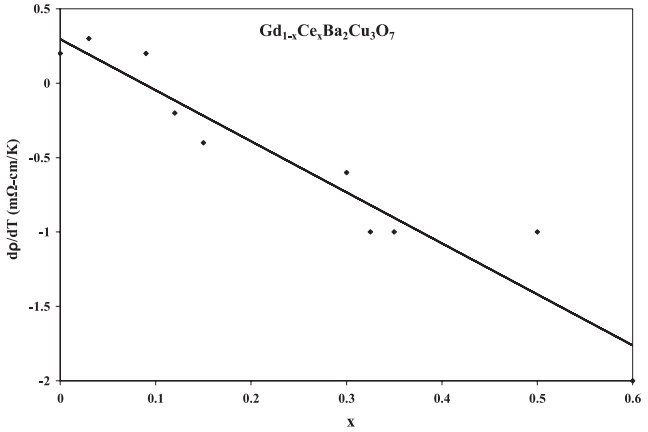

Figure 5. The derivative of the normal state resistivity ($T > 100$) versus x.

a considerable effect upon T_c and superconducting properties. With the increase of x, the normal state resistivity of the samples increase continuously and their slopes change from positive (metal-like) to negative (insulator-like) at the critical level $x_c = 0.12$. For $x > 0.12$, the resistivity curves show the broad maxima just above T_c. This upturn in the resistivity with lowering the temperature is related to MIT which occurs at x_c. With the increase of the number of insulating parts in the grains, the homogeneity of the grains decreases. This leads to both the decrease of T_c and the increase of the normal state resistivity. In other words, it causes an MIT in the normal state. Some more changes also occur at this point which should be considered more thoroughly. As noted above, Ce content enters the lattice in tetravalent or near-tetravalent form; therefore the concentration of carriers decreases with the increase of Ce content and the superconducting state disappears for $x \geqslant 0.7$.

In figure 4, the normal state resistivity $\rho(T)$ of the samples at 273 K is shown as a function of x for the GdCe123 compounds. Throughout the normal state, the resistivity increases as x increases. Changes of the normal state resistivity versus x have two different slopes for low and high values of x, showing a break at $x_c = 0.12$. This behavior, corresponding to MIT in figure 3, has also been observed in other HTSCs [12].

A similar effect was observed in the GdPr123 systems, that the normal state resistivity increases slowly at low values of x and increases faster for $x > 0.35$ [6]. This behavior has also been observed in the normal state resistivity versus oxygen deficiency δ for the deoxygenated system [13]. This abrupt change in the normal state resistivity versus x implies that different conduction mechanisms govern in these two regions.

The derivative of the resistivity, $d\rho/dT$, is sketched as a function of x in figure 5. This scheme is suggested for temperatures higher than T_c in the normal state of the resistivity. The straight line fitted to $d\rho/dT$ versus x shows that the structures of the samples have not changed with the increase of x. By Ce doping in the GdCe123 samples, the onset and the offset transition temperatures decrease, and both the transition temperature width and the normal state resistivity increase. These prove that Ce substitution destroys superconductivity by a hole-filling mechanism in the CuO_2 planes.

Many experimental and theoretical investigations indicate that two-dimensional conductivity regimes govern the conductivity in the normal and superconducting states of HTSC

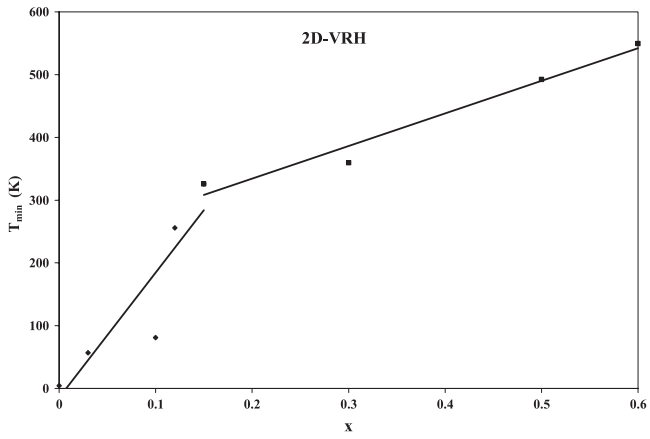

Figure 6. $T_{\min}$ versus x from the results of VRH fitting.

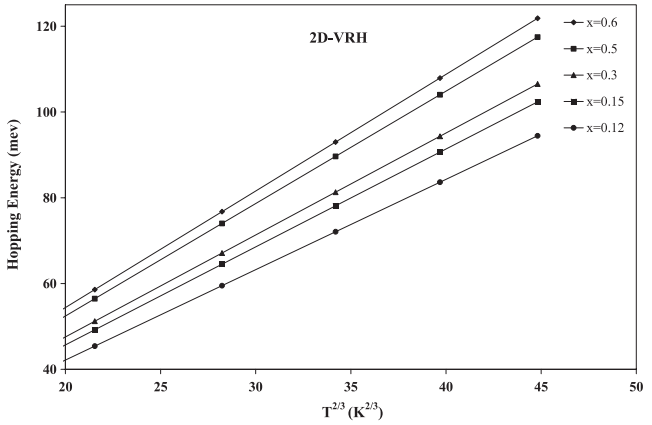

Figure 7. The hopping energy for different values of x versus $T^{2/3}$ in the normal state of the resistivity from VRH results.

materials [3, 14]. In HTSC materials, the coherence length is less than the lattice spacing in the c direction, and then superconductivity occurs predominantly in the CuO_2 planes. Indeed, we need to consider quasi-2D models of these superconductors. The normal resistivity of HTSC materials have been, so far, analyzed with different models. The resistivity data are least squares fitted to $\rho = \rho_0(T/T_0)^{2p}\exp(T_0/T)^p$, where in the variable range hopping (VRH) regime, there is $p = 1/(D+1)$ with D the dimensionality of the conduction mechanism, and in the Coulomb gap (CG) regime, we have $p = 1/2$ in both two and three dimensions. The fitting parameters for the best fitted regime are listed in table 1. The χ^2 parameter, as the squared standard deviation for this fitting, indicates the accuracy of the fitting. As Ce content is increased, the resistivity shows a change from the metallic behavior, $\rho = A + BT$, to the semiconducting behavior, particularly in the low temperature region. These two regions are separated by a shallow minimum, $\rho_{\min}$, at $T_{\min}$. Then $\rho(T)$ has a minimum at $T_{\min} = T_0/2^{1/p}$, where $T_{\min}$ is quite high in the temperature range of the measurements. The absence of $T_{\min}$ in the ρ versus T curve for these samples ($x \geqslant 0.35$) suggests that $T_{\min}$ occurs at higher temperatures (>300 K). Measurements at the higher temperatures have supported this assumption [15]. In the opposite limit, where $T_{\min}$ is very low, only the metallic form can be observed. The data in table 1 shows that, in the GdCe123 samples for $x < 0.12$, the conduction follows the CG regime, whereas for $x \geqslant 0.12$ it follows the 2D VRH mechanism. The calculated $T_{\min}$ for the samples is sketched as a function of x in figure 6. In this curve, a sudden change occurs near $x = 0.12$, which accompanies other changes near this point, corresponding to the MIT.

The fitting parameters show that the fully metallic samples have T_0^{CG} smaller than T_0^{VRH}, and the inverse is true for the fully semiconducting samples. This is an indication of the crossover from $p = 1/2$ to $1/3$, accompanied with both a gradual change of ρ from the metallic state to the semiconducting state and a progressive decrease of the localization length, which is the decay length of the localized wavefunction (d) as a function of doping level x. Using the Mott parameterization [16], the localization length is derived: $d = 16/(k_{\mathrm{B}}T_0N_{2\mathrm{D}}(E_{\mathrm{f}}))$, where k_{B} is the Boltzmann constant

Table 1. Results of VRH fitting for $Gd_{1-x}Ce_xBa_2Cu_3O_{7-\delta}$.

x	p	χ^2	$T_{\min}$ (K)	d (Å)	Best fit
0	0.50	0.9997	4.23	987.59	CG
0.03	0.50	0.9991	56.69	73.59	CG
0.1	0.50	0.9989	80.96	51.54	CG
0.12	0.33	0.9999	255.8	89.06	2D-VRH
0.15	0.33	1	325.8	78.92	2D-VRH
0.3	0.33	0.9999	359.5	74.34	2D-VRH
0.5	0.33	0.9993	492.1	64.21	2D-VRH
0.6	0.33	1	549.4	60.77	2D-VRH

and $N_{2\mathrm{D}}(E_{\mathrm{f}})$ is the DOS at the Fermi level. It has been measured that $N_{2\mathrm{D}}(E_{\mathrm{f}})$ is a few times 10^{12} state cm^{-2} eV^{-1} for different x contents [2, 3, 14, 17]. According to the current estimate of $N_{2\mathrm{D}}(E_{\mathrm{f}}) = 10^{12}$ state cm^{-2} eV^{-1}, the localization length of the samples have been calculated. Both the hopping energy, $E_{2\mathrm{D}} = (k_{\mathrm{B}}T/d)^{2/3}/N_{2\mathrm{D}}(E_{\mathrm{f}})^{1/3}$, the interval of width or the amount of energy needed for hopping at temperature T, and the hopping range, $R_{2\mathrm{D}} = (d/(\pi N_{2\mathrm{D}}(E_{\mathrm{f}})k_{\mathrm{B}}T))^{1/3}$ at temperature T, obey the Mott law [18].

Based on the 2D VRH, the hopping energy, the hopping range and the localization length have been calculated for various x. In figure 7, the hopping energy of GdCe123 for different values of x is sketched as a function of temperature. The hopping energy also increases for higher values of x. The hopping range of the samples for different values of x is shown in figure 8, and in the inset to the figure the localization length versus x is sketched. With the increase of temperature, the hopping range decreases. The decrease of both the localization length and the hopping range and the increase of the hopping energy indicate that doping Ce localizes the holes and suppresses the superconducting state, and also that the carriers need higher energy to hop to the other sites. These points emphasize that the semiconducting state overcomes the normal state of the system after the increase in Ce content. The behavior of the GdCe123 compounds below and above $x_{\mathrm{c}} = 0.12$ according to the different experiments and fittings with the VRH show an MIT in the normal state, which indicates that there are two different mechanisms for conductivity.

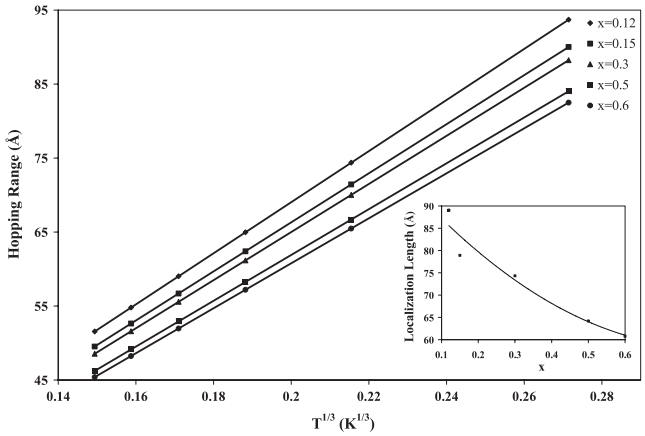

Figure 8. The hopping range for different values of x versus $T^{-1/3}$ in the normal state of the resistivity from the VRH results. The inset is the localization length versus x.

4. Conclusions

We have synthesized a series of $Gd_{1-x}Ce_xBa_2Cu_3O_{7-\delta}$ ceramic samples with various x. we have characterized them by XRD and have performed electrical resistivity measurements in the temperature range 10–300 K. On the basis of the quantum percolation theory with an electron localization mechanism, we interpret the resistivity data for the GdCe123 samples with different Ce doping levels in a wide range of temperatures by means of a single theory. The normal state resistivity of the samples shows that the system undergoes an MIT. For the $x \geqslant 0.12$ samples the conduction follows the 2D VRH mechanism whereas for $x < 0.12$ it shows the CG regime. Increasing the superconductivity transition width shows that Ce doping makes some defects in the Josephson weak links and by producing the impurity phases such as $BaCeO_3$ it makes the intragrain links become weaker.

Acknowledgments

We would like to acknowledge useful discussions with S Mirshamsi, S Fallahi, H Hadipour and H Abbaszadeh. This work was supported in part by the Centre of Excellence in Complex Systems and Condensed Matter (CSCM), Department of Physics, Sharif University of Technology (http://www.cscm.ir/).

References

[1] Li W H, Chuang W H, Wu S Y, Lee K C, Lynn J W, Tsay H L and Yang H D 1997 *Phys. Rev.* B **56** 5631
[2] Yamani Z and Akhavan M 1997 *Phys. Rev.* B **56** 7894
[3] Yamani Z and Akhavan M 1998 *Solid State Commun.* **107** 197
[4] Akhavan M 2002 *Physica* B **321** 265
[5] Akhavan M 2004 *Phys. Status Solidi* b **241** 1242
[6] Mohammadizadeh M R and Akhavan M 2003 *Phys. Rev.* B **68** 104516
[7] Staub U, Antinio M R and Solderholm L 1994 *Phys. Rev.* B **50** 7085
[8] Cao G, Bolivar J, O'Rielly J W, Crow J E, Kennedy R J and Pernambuco P 1993 *Physica* B **186** 1004
[9] Fincher C R and Blanchet G B 1991 *Phys. Rev. Lett.* **67** 2902
[10] Gnanasekar K I, Tamhane A S, Gupta L C, Pai S P, Apte P R, Sharon A and Vijayaraghavan R 1995 *Phys. Rev.* B **52** 1362
[11] Shi L, Huang Y, Pang W, Liu X, Wang L, Li X, Zhou G and Zhang Y 1997 *Physica* C **282** 1021
[12] Akhavan M 1995 *Physica* C **250** 25
[13] Krylov K R, Ponomarev A I, Tsidilkovski I M, Tsidilkovski V I, Bazuev G V, Kozhevnikov V L and Cheshniski S M 1988 *Phys. Rev.* A **131** 203
[14] Mohammadizadeh M R and Akhavan M 2003 *Supercond. Sci. Technol.* **16** 1216
[15] Osquiguil E J, Cival L, Decca R and De la Cruz F 1988 *Phys. Rev.* B **38** 2840
[16] Mott N F and Davis E A 1979 *Electronic Process in Non-Crystal Materials* 2nd edn (Oxford: Clarendon)
[17] Kabasawa U, Tarutani Y, Okamoto M, Fukazawa T, Tsukamoto A, Hiratani M and Takagi K 1993 *Phys. Rev. Lett.* **70** 1700
[18] Kaveh N and Mott N F 1992 *Phys. Rev. Lett.* **68** 1904